High performance InP ring resonator for new generation monolithically integrated optical gyroscopes

Caterina Ciminelli,[1,*] Francesco Dell'Olio,[1] Mario N. Armenise,[1] Francisco M. Soares,[2,3] and Wolfgang Passenberg[2]

[1]*Optoelectronics Laboratory, Politecnico di Bari, ViaOrabona 4, 70125 Bari, Italy*
[2]*Fraunhofer Institute for Telecommunications, Heinrich-Hertz-Institut, Einsteinufer 37, 10587 Berlin, Germany*
[3]*francisco.soares@hhi.fraunhofer.de*
[*]*c.ciminelli@poliba.it*

Abstract: An InP ring resonator with an experimentally demonstrated quality factor (Q) of the order of 10^6 is reported for the first time. This Q value, typical for low loss technologies such as silica-on-silicon, is a record for the InP technology and improves the state-of-the-art of about one order of magnitude. The cavity has been designed aiming at the Q-factor maximization while keeping the resonance depth of about 8 dB. The device was fabricated using metal-organic vapour-phase-epitaxy, photolithography and reactive ion etching. It has been optically characterized and all its performance parameters have been estimated. InP waveguide loss low as 0.45 dB/cm has been measured, leading to a potential shot noise limited resolution of 10 °/h for a new angular velocity sensor.

OCIS codes: (230.5750) Optical devices; (130.0130) Integrated optics; (130.3120) Integrated optics devices; (130.6010) Sensors; (060.2800) Gyroscopes; (140.3370) Laser gyroscopes.

References and links

1. M. N. Armenise, C. Ciminelli, F. Dell'Olio, and V. M. N. Passaro, *Advances in Gyroscope Technologies* (Springer, 2010), chaps. 3–4.
2. C. Ciminelli, F. Dell'Olio, C. E. Campanella, and M. N. Armenise, "Photonic technologies for angular velocity sensing," Adv. Opt. Photon. **2**(3), 370–404 (2010).
3. O. Kenji, "Semiconductor ring laser gyro," Japanese patent # JP 60,148,185, filed 1984, issued 1985.
4. M. Armenise and P. J. R. Laybourn, "Design and Simulation of a Ring Laser for Miniaturised Gyroscopes," Proc. SPIE **3464**, 81–90 (1998).
5. M. N. Armenise, V. M. N. Passaro, F. De Leonardis, and M. Armenise, "Modeling and Design of a Novel Miniaturized Integrated Optical Sensor for Gyroscope Systems," J. Lightwave Technol. **19**(10), 1476–1494 (2001).
6. M. Osiński, H. Cao, C. Liu, and P. G. Eliseev, "Monolithically integrated twin ring diode lasers for rotation sensing applications," J. Cryst. Growth **288**(1), 144–147 (2006).
7. W. Lawrence, "Thin film laser gyro," US Patent 4326803, filed 1979, issued 1982.
8. K. Suzuki, K. Takiguchi, and K. Hotate, "Monolithically integrated resonator microoptic gyro on silica planar lightwave circuit," J. Lightwave Technol. **18**(1), 66–72 (2000).
9. H. Mao, H. Ma, and Z. Jin, "Polarization maintaining silica waveguide resonator optic gyro using double phase modulation technique," Opt. Express **19**(5), 4632–4643 (2011).
10. C. Ciminelli, F. Dell'Olio, C. E. Campanella, and M. N. Armenise, "Numerical and experimental investigation of an optical high-Q spiral resonator gyroscope," Proc. 14th Transparent Optical Networks (ICTON), Coventry, UK, Jul 2 - 5, 2012. DOI: 10.1109/ICTON.2012.6254463.
11. C. Ciminelli, F. Dell'Olio, and M. N. Armenise, "High-Q spiral resonator for optical gyroscope applications: numerical and experimental investigation," IEEE Photon. J. **4**(5), 1844–1854 (2012).
12. G. Li, K. A. Winick, B. R. Youmans, and E. A. J. Vikjaer, "Design, fabrication and characterization of an integrated optic passive resonator for optical gyroscopes," presented at Institute of Navigation's 60th Annual Meeting, Dayton, Ohio, USA, June 7–9, 2004.
13. L. Guo, B. Shi, C. Chen, and M. Zhao, "A large-size SiO_2 waveguide resonator used in integration optical gyroscope," Optik (Stuttg.) **123**(4), 302–305 (2012).
14. M. Smit, J. van der Tol, and M. Hill, "Moore's law in photonics," Laser Photon. Rev. **6**(1), 1–13 (2012).

#177994 - $15.00 USD Received 16 Oct 2012; revised 21 Dec 2012; accepted 21 Dec 2012; published 7 Jan 2013

15. V. I. Tolstikhin, A. Densmore, Y. Logvin, K. Pimenov, F. Wu, and S. Laframboise, "44-channel optical power monitor based on an echelle grating demultiplexer and a waveguide photodetector array monolithically integrated on an InP substrate," Proceedings of the Optical Fiber Communication Conference OFC 2003, Atlanta, Georgia, USA, 2003, paper PD37.
16. R. Nagarajan, M. Kato, J. Pleumeekers, P. Evans, D. Lambert, A. Chen, V. Dominic, A. Mathur, P. Chavarkar, M. Missey, A. Dentai, S. Hurtt, J. Bäck, R. Muthiah, S. Murthy, R. Salvatore, S. Grubb, C. Joyner, J. Rossi, R. Schneider, M. Ziari, F. Kish, and D. Welch, "Single-chip 40-channel InP transmitter photonic integrated circuit capable of aggregate data rate of 1.6 Tbit/s," Electron. Lett. **42**(13), 771–773 (2006).
17. S. Nicholes, M. L. Mašanovic, B. Jevremovic, E. Lively, L. Coldren, and D. J. Blumenthal, "The World's First InP 8x8 Monolithic Tunable Optical Router (MOTOR) Operating at 40 Gbps Line Rate per Port," Optical Fiber Communication ConferenceOFC 2009, San Diego, CA, USA, 2009, paper PDPB1.
18. F. M. Soares, N. K. Fontaine, R. P. Scott, J. H. Baek, X. Zhou, T. Su, S. Cheung, Y. Wang, C. Junesand, S. Lourdudoss, K. Y. Liou, R. A. Hamm, W. Wang, B. Patel, L. A. Gruezke, W. T. Tsang, J. P. Heritage, and S. J. B. Yoo, "Monolithic InP 100-Channel × 10-GHz Device for Optical Arbitrary Waveform Generation," IEEE Photon. J. **3**(6), 975–985 (2011).
19. C. Ciminelli, F. Dell'Olio, V. M. N. Passaro, and M. N. Armenise, "Low-loss InP-based ring resonators for integrated optical gyroscopes," presented at Caneus 2009 Workshop, NASA Ames Center, Moffett Field, CA, USA, March 1–6, 2009.
20. F. Dell'Olio, C. Ciminelli, V. M. N. Passaro, and M. N. Armenise, "Optical angular velocity sensors and related read-out systems for new generation gyroscopes," presented at 1st Networking/Partnering Day 2010, Noordwijk, Nederland, January 28, 2010.
21. G. A. Sanders, M. G. Prentiss, and S. Ezekiel, "Passive ring resonator method for sensitive inertial rotation measurements in geophysics and relativity," Opt. Lett. **6**(11), 569–571 (1981).
22. C. Ciminelli, F. Dell'Olio, C. E. Campanella, V. M. N. Passaro, and M. N. Armenise, "Integrated Optical Ring Resonators: Modelling and Technologies," in *Progress in Optical Fibers*, P. S. Emersone, Ed. (Nova Science Publisher, 2010).
23. S. J. Choi, K. Djordjev, Z. Peng, Q. Yang, S. J. Choi, and P. D. Dapkus, "Laterally Coupled Buried Heterostructure High-Q Ring Resonators," IEEE Photon. Technol. Lett. **16**(10), 2266–2268 (2004).
24. F. Dell'Olio, C. Ciminelli, M. N. Armenise, F. M. Soares, and W. Rehbein, "Design, fabrication, and preliminary test results of a new InGaAsP/InP high-Q ring resonator for gyro applications," 24th International Conference on Indium Phosphide and Related Materials, Santa Barbara, CA, USA, August 27–30, 2012.
25. C. Ciminelli, V. M. N. Passaro, F. Dell'Olio, and M. N. Armenise, "Three-dimensional modelling of scattering loss in InGaAsP/InP and silica-on-silicon bent waveguides," J. European Opt. Soc. Rapid Publications **4**, 09015 (2009).
26. R. Regener and W. Sohler, "Loss in Low-Finesse Ti:$LiNbO_3$ Optical Waveguide Resonators," Appl. Phys. B **36**(3), 143–147 (1985).
27. A. Yariv, "Universal relations for coupling of optical power between microresonators and dielectric waveguides," Electron. Lett. **36**(4), 321–322 (2000).

1. Introduction

Optoelectronic gyroscopes available on the market, i.e. ring laser gyro (RLG) and fiber optic gyro (FOG), are well established sensors widely utilized in the field of inertial navigation of civil and military vehicles, including satellites, airplanes, and helicopters [1]. Although they have outstanding performance (resolution < 0.1 °/h), those rotation sensing systems are too bulky and power consuming for some emerging applications demanding low-power and reliable miniaturized gyros. To effectively respond to this increasing market demand, integrated optoelectronic angular velocity sensors are emerging as a promising alternative to the RLG and the FOG [2].

Integrated optical gyros are all based on a planar cavity, either active or passive, supporting two resonant modes having the same resonance order. According to the Sagnac effects, resonance frequencies of those modes are split by rotation and their difference is proportional to the angular velocity Ω. Measuring this difference through an appropriate readout optoelectronic system, Ω can be estimated with very high accuracy.

Miniaturized gyroscopes based on semiconductor ring lasers [3–6] are very interesting devices with a footprint < 100 mm^2 and a theoretical resolution comparable to that one of RLGs but, until now, their experimental demonstration has been prevented by the lock-in effect and the mode competition between the counter-propagating resonant modes.

Resonant micro optical gyros (RMOGs) based on passive resonators were conceptually envisaged at the end of the 70s [7] and are now considered with increasing attention

#177994 - $15.00 USD Received 16 Oct 2012; revised 21 Dec 2012; accepted 21 Dec 2012; published 7 Jan 2013

especially for those application domains (e.g. rover vehicles navigation or telecom satellites attitude control) requiring medium performance (resolution of a few tens of °/h).

RMOG prototypes successfully demonstrated in the last few years [8–11] include a high-Q ($\geq 10^6$) resonator (sensing element) fabricated by a low loss technology, e.g. glass [12] and silica-on-silicon [13], and some optoelectronic components (laser, splitter, modulators, photodiodes) for the cavity excitation and the sensor readout. Since the resonator and the other gyro components are realized on different substrate materials, they can only be integrated by hybrid approaches (e.g. Silicon Optical Bench technology).

Recent progress of the InP PICs (photonic integrated circuits) technology [14] with the demonstration of very complex monolithically integrated devices such as WDM (wavelength division multiplexing) transmitters/receivers [15,16], WDM routers [17], and arbitrary waveform generators [18], has suggested the idea of a fully integrated InP gyroscope [19,20] with a target resolution of the order of 10 °/h.

The shot noise limited resolution $\delta\Omega$ of RMOGs based on a ring resonator strongly depends on both the cavity quality factor Q and the ring diameter d, being equal to [21]:

$$\delta\Omega = \frac{\sqrt{2}\,c}{Q\,d} Z \tag{1}$$

where

$$Z = \sqrt{Bh\,\nu_0 / \eta_{pd} P_{pd}} \tag{2}$$

c is the speed of light in vacuum, B is the sensor bandwidth, h is the Planck constant, ν_0 is the gyro operating frequency (= 193 THz, corresponding to the operating wavelength of 1.55 μm), η_{pd} is the quantum efficiency of the photodiodes included in the readout optoelectronic system, and P_{pd} is the average optical power at the photodiodes input.

In Fig. 1, the dependence of $\delta\Omega$ on the ring diameter d and quality factor Q is shown in terms of level curves, assuming B = 1 Hz, η_{pd} = 0.9 and P_{pd} = 1 mW. As it can be observed from Fig. 1, a resolution improvement can be obtained by increasing Q and/or d and the achievement of the target resolution ($\delta\Omega$ = 10 °/h, red level curve) requires $Q \geq 10^6$ and d ≥ 10 mm.

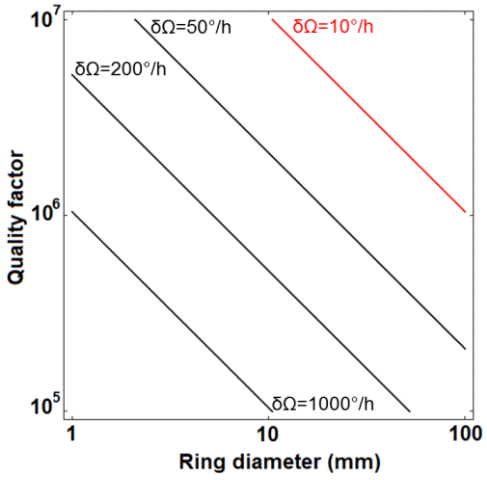

Fig. 1. Gyro resolution dependence on d and Q in terms of level curves. Log scale has been used for both axes.

Typical values of the Q-factor of InP resonators are in the range $10^3 \div 10^5$ [22] and the best performing InP ring resonator so far reported exhibits a quality factor of 113,000, with a

#177994 - $15.00 USD Received 16 Oct 2012; revised 21 Dec 2012; accepted 21 Dec 2012; published 7 Jan 2013

ring radius of 0.2 mm (waveguide propagation loss = 1.7 dB/cm) [23]. As shown in Fig. 1, features of InGaAsP/InP rings are currently incompatible with an RMOGs target resolution of 10 °/h, and a considerable improvement of the state-of-the-art is needed for the practical realization of an InP-based gyro-on-a-chip, GoC (fully monolithically integrated RMOG), with the performance demanded by the market.

In this paper we report on design, fabrication and optical characterization of an InGaAsP/InP ring resonator with Q equal to 0.97 x 10^6. The measured quality factor improves of about one order of magnitude the state-of-the-art and experimentally demonstrates the potential feasibility of a GoC with a resolution of a few tens of °/h. The device we propose in this paper is about 30% more performing than the resonator we described in Ref [24].

2. Resonator configuration and design criteria

The configuration of the fabricated ring resonator is shown in Fig. 2(a). It includes just one bus waveguides instead of two to enhance the cavity quality factor, which strongly influences the gyro resolution. The ring radius (= 13 mm) has been chosen so that the device fits in ¼ of the 3-inch InP wafer. This design strategy assures a good uniformity of the fabrication process.

For the resonator fabrication, a low-loss InGaAsP/InP rib waveguide with etch depth h = 0.3 μm and width w = 2.0 μm (as shown in Fig. 2(b)) has been selected. The choice of the geometrical dimension and the index contrast of the guiding structures is the result of a compromise between the scattering loss reduction, demanding the decrease of the etch depth and the increase of the width, and the bending loss minimization which requires the increase of both h and the index contrast. Further details on the waveguide are in [24].

To enhance the coupling between the straight bus waveguide and the fiber pigtails connected to the bus ends we have designed two tapers at the two bus ends, which have been simulated by the 3D beam propagation method (BPM) [24]. BPM simulations show that losses due to the propagation within the taper are less than 1% and the overlap integral between the taper output field and the field of a standard single mode fiber is equal to 22%.

The propagation loss α of the fundamental quasi-TE mode supported by the single-mode guiding structure, which has been estimated by the 3D model proposed in [25] based on the volume current method, is in the range 0.45 ÷ 1.0 dB/cm. Propagation loss of the fundamental quasi-TM mode is > 1 dB/cm. Therefore only the quasi-TE mode, which exhibits a confinement factor > 80%, has been considered in our study. The effective index n_{eff} of that mode, calculated by the 3D finite element method, is 3.205.

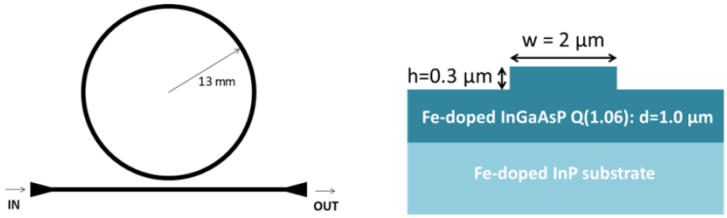

Fig. 2. Configuration of the fabricated device.

The gap between the ring resonator and the straight bus waveguide, which determines the efficiency η_c of the bus/cavity coupler, has been identified by imposing a resonance depth of 8 dB. We have optimized the coupler efficiency aiming at the fulfillment of this constraint. Since the result of the optimization procedure depends on the assumed value, we have considered four values of the propagation loss, i.e. 0.50 dB/cm, 0.65 dB/cm, 0.80 dB/cm, and 0.95 dB/cm. To assure a uniform step (= 0.15 dB/cm) between those values we have not

#177994 - $15.00 USD Received 16 Oct 2012; revised 21 Dec 2012; accepted 21 Dec 2012; published 7 Jan 2013

considered both the maximum and the minimum of the α variation range (i.e., 1.0 and 0.45 dB/cm, respectively).

For the assumed α values, we have derived the relevant values of both the optimum efficiency and the optimum gap. The selected values of the gap and the coupling efficiency are g_1 = 1.739 μm, 34.1%, g_2 = 1.620 μm, 42.3%, g_3 = 1.524 μm, 49.9%, and g_4 = 1.444 μm, 56.9%, respectively. Thus we have fabricated four resonators having the same ring radius (i.e. 13 mm) and the four optimized values of the gap. Since each resonator fits in ¼ of the 3-inch wafer, the four devices have been fabricated on the same wafer. Further details on the resonators design are in [24].

3. Resonator fabrication

The four ring resonators have been fabricated using a single standard-lithography process and the 1μm InGaAsP Q(1.06μm) guiding layer has been grown on top of an InP substrate by metal-organic vapour-phase-epitaxy (MOVPE). Both the InP substrate and the Q(1.06) layer are electrically non-conductive (i.e., Fe-doped), in order to eliminate free-carrier optical absorption on the waveguides. The waveguides have been anisotropically etched in a reactive-ion etcher using a thin silicon-nitride layer as mask. All the waveguide structures have been patterned using just one standard lithography. After processing, the wafer has been cleaved and an anti-reflection coating has been deposited at the input and output waveguide facet of the ring resonator.

The four fabricated chips are shown in Fig. 3(a) and each of them has a footprint of about 700 mm^2. Each chip includes three test waveguides with a length of 6.7 mm, 11.7 mm, and 21.0 mm. Figure 3(b) shows an SEM image of the waveguide structure at the facet of each chip.

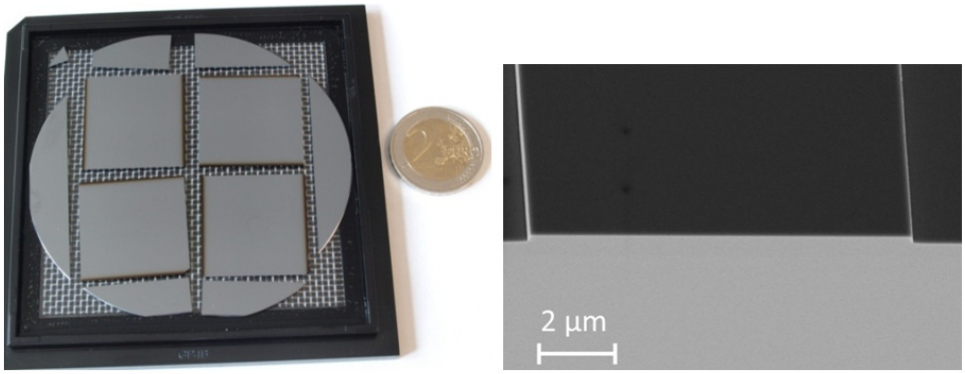

Fig. 3. Photograph of the cleaved 3-inch InP wafer on a GelPak including the four AR-coated ring-resonator chips in the middle a), and an SEM image of the 300nm-high waveguide at the facet of the chips b).

Two sections of the bus/cavity coupler of a fabricated resonator are shown in Fig. 4. The SEM image in Fig. 4(a) shows the section in which the distance between the ring and the straight bus waveguide is minimum. In Fig. 4(b) we show another section of the coupler, where the distance between the waveguides is higher.

SEM images show also that the waveguide of the fabricated devices is 10% wider than the designed one. Both numerical simulations based on the coupled mode theory and optical characterization confirmed that the actual coupling efficiency is lower than the expected one. The efficiency reduction is in the range 20% - 25% for the considered gap values and decreases as the gap decreases.

#177994 - $15.00 USD Received 16 Oct 2012; revised 21 Dec 2012; accepted 21 Dec 2012; published 7 Jan 2013

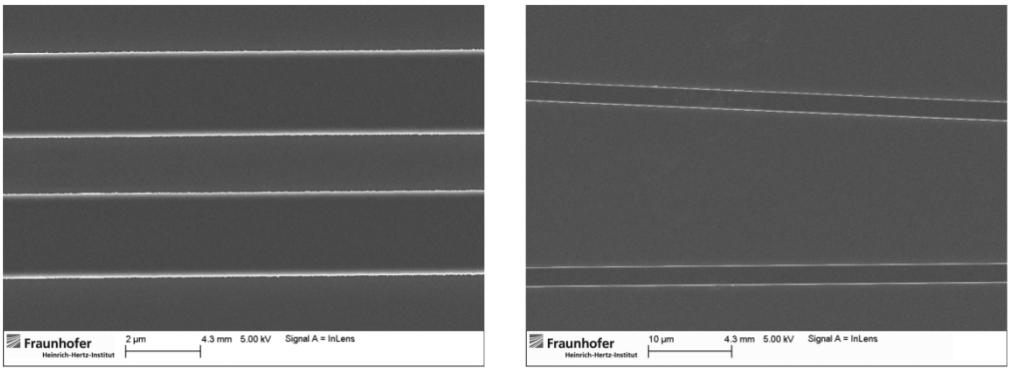

Fig. 4. Top view of two sections of the cavity/bus couplers obtained through the scanning electron microscope (SEM).

4. Optical characterization of the waveguide and the resonator

First of all we have experimentally estimated the propagation loss of the TE mode propagating within the rib waveguide by using the method in [26]. Due to the reflectivity R (= 31%) of the air/waveguide interface, each test waveguide is a Fabry-Perot cavity whose spectral response has been measured by a tunable laser and a photodetector connected to an oscilloscope (see the measurement setup, which includes also a polarization controller, in Fig. 5).

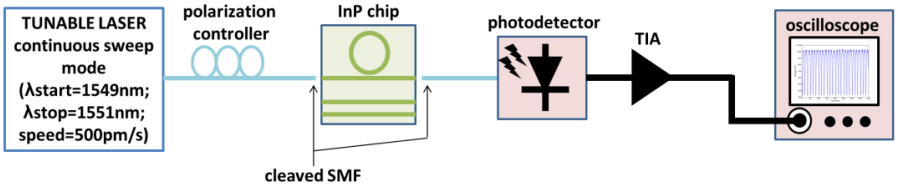

Fig. 5. Setup for the measurement of the waveguide propagation loss and the ring resonators TIA: transimpedance amplifier.

The laser continuously scans the wavelength from 1.549 µm to 1.551 µm with a speed of 500 pm/s and the time-varying output optical intensity is measured by the photodetector and recorded by the oscilloscope.

For example, in Fig. 6 we show the cavity spectrum measured on a test straight waveguide having a length L = 21.0 mm. All the adjacent fringes are identical to that one in Fig. 6. We verified that the fringes adjacent to the shown one are identical. The measured cavity free spectral range (FSR) is 17.8 pm, which is quite close to the FSR value (16.9 pm) numerically evaluated by taking into account the material dispersion. The normalized output intensity ranges from 1 to 0.37.

#177994 - $15.00 USD Received 16 Oct 2012; revised 21 Dec 2012; accepted 21 Dec 2012; published 7 Jan 2013

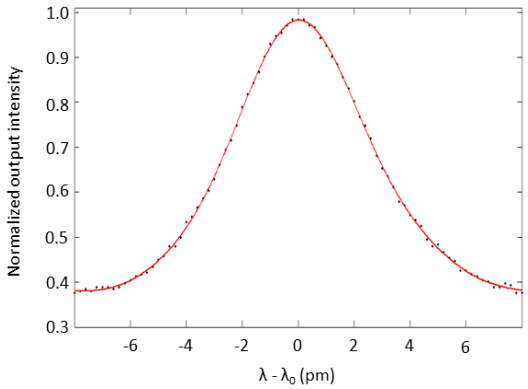

Fig. 6. Spectrum of the Fabry-Perot cavity including the 21 mm long test waveguide.

The waveguide propagation loss (in dB/cm, if L is expressed in cm) is given by [26]:

$$\alpha = \frac{4.34}{L}\left\{\ln R - \ln\left[\frac{1}{K}\left(1-\sqrt{1-K^2}\right)\right]\right\} \tag{3}$$

where

$$K = \frac{I_{max} - I_{min}}{I_{max} + I_{min}} \tag{4}$$

I_{max} and I_{min} are the maximum an the minimum of the cavity spectral response.

For the 21.0 mm long test waveguide the measured propagation loss is 0.50 dB/cm. We have measured, with the described procedure, the propagation loss of each test waveguide. The test waveguides having length = 11.7 mm and 6.7 mm exhibit a propagation loss of 0.44 dB/cm and 0.40 dB/cm, respectively. The average α value is then 0.45 dB/cm. The standard deviation of the measured α values is 9% of the average value.

The spectral response of all the fabricated resonators has been measured using the setup in Fig. 5, with the laser wavelength sweeping continuously from 1.549 μm to 1.551 μm.

The best performing resonator is that one having a bus/cavity gap g_3 = 1.524 μm. The other fabricated resonators have a quality factor of the order of $10^4 \div 10^5$. The preliminary characterization of one of them, which has a gap g_4 = 1.444 μm and Q = 740,000, has been reported in [24].

The resonator with a bus/cavity gap g_1 = 1.739 μm has exhibited a real value of the coupler efficiency close to 9% which is about 25% lower than the designed one. Therefore its resonance depth is about 2 dB and it is not useful for our specific application.

The normalized spectral response of the best performing device is in Fig. 7. We have measured 24 resonances and the resonator performance in Table 1 is averaged over all them. The slight non-uniformity (the standard deviation is < 10% of the mean value) observed in the Q-factor of the 24 resonances is due to the non-constant speed of the laser sweep.

The quality factor is very close to 1×10^6 and thus is about 8.5 times larger than the state-of-the-art [22]. The measured value of Q is quite close to the intrinsic Q, which is equal to 1.24×10^6.

The measured resonance depth is 7.0 dB. The difference between the numerical and experimental values of the resonance depth may be due to the fabrication tolerance on the gap value.

#177994 - $15.00 USD Received 16 Oct 2012; revised 21 Dec 2012; accepted 21 Dec 2012; published 7 Jan 2013

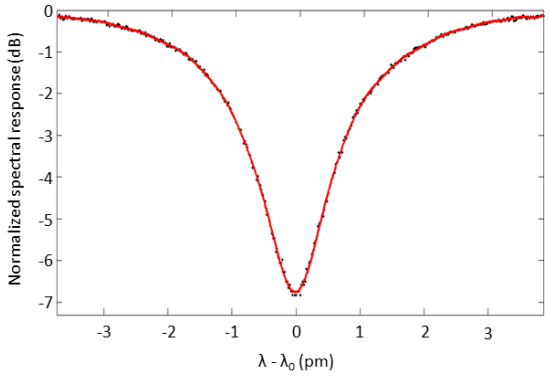

Fig. 7. Spectral response of the resonator with gap g_3 = 1.524 µm(best performing device).

Table 1. Performance of the resonator with gap g_3 = 1.524 µm(best performing device).

Performance parameter	Value
Resonance depth (dB)	7.0
Free spectral range (pm)	8.4
Full width at the half maximum (pm)	1.6 pm
Quality factor	0.97 x 10^6
Finesse	5.3
Waveguide propagation loss	0.45 dB/cm
Efficiency of the bus/cavity coupler	27.7%

The well-known expression of the spectral response of a ring resonator coupled to one bus waveguide [27] has been used to fit experimental data of the spectrum by a nonlinear curve-fitting technique. The parameters of the best fitting curve are α = 0.44 dB/cm and η_c = 27.7%. The α value is in very good agreement with that one experimentally obtained, i.e. α = 0.45 dB/cm.

5. Gyro resolution

By using Eq. (1) the shot noise limited resolution of the RMOG including the best performing InP ring resonator can be predicted. In Fig. 8 the dependence of the resolution $\delta\Omega$ on the average power at photodiodes input is shown. The resolution is enhanced by a P_{pd} increase and $\delta\Omega$ values of a few tens of °/h are achievable for $P_{pd} \geq 1$ mW. For P_{pd} = 1 mW the resolution is about 40 °/h. The performance $\delta\Omega$ = 10 °/h is obtained for P_{pd} = 13.84 mW. Commercial photodiodes have a saturation power up to 20 mW and thus P_{pd} values of a few tens of mW are realistically achievable.

The measured quality factor is already very high for the InP technology but a further decrease of the waveguide propagation loss of 20% (down to 0.36 dB/cm) can increase the quality factor up to 1.13 x 10^6 with a consequent resolution improvement of 16% (for example, the resolution is 35 °/h for P_{pd} = 1 mW and 8.8 °/h for P_{pd} = 13.84 mW).

The increase of the ring radius of 20% (up to 15. 6 mm) has a negligible effect of the ring quality factor but it has a beneficial effect on the sensor resolution which is about 30 °/h for P_{pd} = 1 mW and 8.3 °/h for P_{pd} = 13.84 mW. Unfortunately, the increase of the chip footprint could imply a degradation of the uniformity of the fabrication process.

#177994 - $15.00 USD Received 16 Oct 2012; revised 21 Dec 2012; accepted 21 Dec 2012; published 7 Jan 2013

To achieve a resolution of 10 °/h with P_{pd} = 1 mW, the radius should be 25 mm and the waveguide propagation loss should be decreased down to 0.25 dB/cm. With those features of the cavity, the resolution reaches 3.3 °/h if P_{pd} = 13.84 mW.

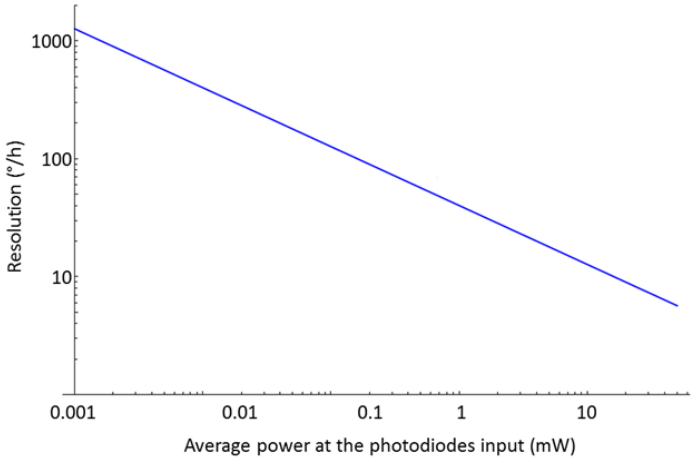

Fig. 8. Resolution of the RMOG based on the best performing fabricated ring resonator vs. the average power optical at the photodiodes input.

6. Conclusions

A large radius InP resonator with a record Q-factor of 0.97 x10^6 has been designed, fabricated, and characterized. The design allows the quality factor maximization and the achievement of a resonance depth compatible with the application. The fabrication process, including metal-organic vapour-phase-epitaxy, photolithography and reactive ion etching, is quite standard and relatively low-cost. The characterization setup is based on a tunable laser whose frequency has been swept in a continuous sweep mode.

The InP waveguide exhibits an experimentally measured propagation loss of 0.45 dB/cm, and the cavity finesse is 5.3 with a resonance depth of 7 dB.

The demonstrated value of the quality factor improves the state-of-the-art of almost one order of magnitude and proves the feasibility of an InP photonic integrated circuit for angular velocity sensing with a resolution of 10 °/h. A further improvement of the sensor performance is achievable by increasing the ring radius and/or minimizing the waveguide propagation loss.

Packaging of fabricated components is currently ongoing and the readout optoelectronic system of the gyroscope has already been designed, fabricated, and tested.

#177994 - $15.00 USD Received 16 Oct 2012; revised 21 Dec 2012; accepted 21 Dec 2012; published 7 Jan 2013